Contribution of Building-Block Test to Discover Unexpected Failure Modes

Taiki Matsumura[1], Raphael T. Haftka[2] and Nam H. Kim[3]
University of Florida, Gainesville, FL, 32611

While the accident rate of airplanes has decreased over decades, accidents still occur mainly due to unexpected failure modes. The objective of this paper is to model in the probabilistic design framework how unexpected failure modes affect reliability, and how post-design tests, called the Building-Block tests, contribute to discovering them. The probabilistic design approach can provide designers and decision-makers with stochastic insight on reliability, i.e., probability of failure. Designers model epistemic and aleatory uncertainties by assuming that they follow certain distributions. However, the current approach does not include the effect of unexpected failure modes, which is the major contributor to most accidents. In the paper, unexpected failure modes are modeled using a large error in epistemic uncertainty, and hierarchical design and test processes to detect them are proposed, as well as a simulation procedure to calculate the associated probability of failure. As an example problem, it is shown that ignoring the effect of unexpected failure modes yields an unconservative estimate of probability of failure by orders of magnitude. It is also shown that the Building-Block test under ultimate load conditions compensates significantly for such unexpected modes, and is effective for discovering modes associated with large errors.

Nomenclature

A	=	Cross-sectional area of structural element
A_{design}	=	Designed cross-sectional area of structural element
A_{test}	=	Cross-sectional area of test specimen of structural element
e_A	=	Error in geometry (area of element) due to manufacturing between design value and actual average
e_{exp}	=	Designer's expected error in stress calculation
e_{true}	=	True error in stress calculation
$e_{P,cal}$	=	Error in internal load calculation in assembled structure
$e_{P,pred}$	=	Error in predicting flight load
e_{test}	=	Error in test configuration and measurement of test load
e_{α}	=	Error in failure theory
e_{σ}	=	Error in stress calculation of structural element
$e_{\sigma f}$	=	Error in predicting material or element strength
G	=	Limit state function
k_d	=	Knockdown factor corresponding material allowable strength
N_{design}	=	Number of possible design outcomes
N_E	=	Number of element tests
P	=	Load on structural element
P_{cal}	=	Calculated maximum flight load on structural element
P_{req}	=	Required load for structural element

[1] Graduate Research Assistant, Mechanical and Aerospace Engineering Department, University of Florida, P.O.Box 116250, Gainesville, FL, 32611-6250, AIAA Student Member
[2] Distinguished Professor, Mechanical and Aerospace Engineering Department, University of Florida, P.O.Box 116250, Gainesville, FL, 32611-6250, AIAA fellow.
[3] Associate professor, Mechanical and Aerospace Engineering Department, University of Florida, P.O.Box 116250, Gainesville, FL, 32611-6250, AIAA member.

P_{tol}	=	Load tolerance
P_{true}	=	True maximum flight load of structural element
P_{ULT}	=	Ultimate load
SF	=	Factor of safety on loads
v_A	=	Variability in geometry (element area) due to manufacturing
v_P	=	Variability in flight load
$v_{\sigma f}$	=	Variability in material or element strength due to material property
α_{true}	=	Coefficient converting material uniaxial strength to structural element strength (true failure theory)
σ_{cal}	=	Calculated stress
σ_{exp}	=	Designer's expected stress
σ_{true}	=	True stress
$\sigma_{f,allow}$	=	Design allowable (strength) of material or element
$\sigma_{f,cal}$	=	Calculated mean of material or element strength
$\sigma_{f,test}$	=	Material or element strength of test specimen
$\sigma_{f,test,obs}$	=	Observed material or element strength of test specimen
$\sigma_{f,true}$	=	True mean of material or element strength

Subscripts:

(A)	=	Assembled structure level
(M)	=	Material level
(E)	=	Element level
$,exp$	=	Designer's expected values (random variables)
$,true$	=	True value (single value)

I. Introduction

A key concept for ensuring reliability of airplane and space vehicles is to understand and predict uncertainties in the systems and operation; uncertainties should be appropriately controlled and managed throughout the entire lifecycle. High-fidelity simulations, such as FEA (Finite Element Analysis), CFD (Computational Fluid Dynamics), etc., have greatly contributed to improving accuracy of predicting flight conditions and structural behaviors. Systematic management tools, such as FMEA (Failure Mode and Effects Analysis), help engineers address potential failure modes effectively. However, airplane accidents and mission failures for space vehicles still occur mainly due to unexpected failure modes. For example, the Aloha Airlines accident in 1988 [1] revealed that multi-site fatigue crack significantly threatened airplane safety, and was followed by a number of investigations and research on this issue. Similarly, the disasters of the Space Shuttle in 1983 and 2001 were also due to unexpected failure scenarios.

Design errors leading to unexpected failure occur due to several causes. Analytical models may have substantial errors. A designer could fail to address even a well-known failure mode. When developing a new product, a lack of knowledge and experience increases risk of design errors. Also, designers might simply make mistakes in modeling, calculation, documentation and so on. Traditionally, a factor of safety is used in order to compensate for uncertainties. However, a factor of safety may not suffice to compensate for unexpectedly large error or unexpected flight event. Critical design error can cause catastrophic failures, and in turn, result in significant consequences. Catastrophic failures during flight directly lead to fatalities. Schedule delay of development due to technical trouble leads to loss of business and increases expenditures on the project. Thus, uncovering unexpected failure modes as early as possible in development is critical to reduce business risk.

Testing is one way of uncovering unexpected failure modes. Building-Block tests (Fig. 1) are commonly employed in aircraft and space vehicle development and are known to effectively reduce technical risk and development cost. The key philosophy of Building-Block tests is that discrepancy between analytical prediction and actual structural behavior is to be found as early as possible. As development proceeds, structural complexity increases. The lower the structural complexity, the more easily failure cause can be identified and isolated. Also, at lower complexity, cost of making test specimens is lower, so that statistical knowledge about structural integrity can be obtained efficiently with a large number of specimens, such as material property distribution. More importantly, detecting technical risk at earlier stage significantly reduces project and business impact. When an unexpected critical failure is found at a later stage, for example at the system certification test, redesign across the system and schedule delay will be inevitable, and in turn, will have a severe impact on the project.

Detailed guidelines of the Building-Block approach for structural design are provided in the Department of Defense Handbook [2], and many aviation applications have been reported. In NASA, the Building-Block approach was successfully applied for Advanced Composites Technology Program (ACT) and High Speed Research Program (HSR) [3]. For a commercial use, the structural certification process of Boeing-777 is presented in Ref. [4].

With growing interest in applying probabilistic design methods to structural reliability [5], researchers also value tests as uncertainty reduction measures (Ref. [6-8]). Probabilistic design frameworks stochastically deal with the epistemic and aleatory uncertainties, and expresses reliability of structure as probability of failure. Recently, Acar et al. [9] explored the contribution of the number of tests at various structural complexities, such as coupon and element tests, to reliability improvement and lifecycle cost. Villanueva et al. [10] showed that a single post-design test of a thermal protection system for space vehicles followed by redesign can dramatically reduce the probability of failure. Urbina et al. [11] proposed a method of uncertainty identification and resource allocation of complex system that is built in a hierarchical way with additional knowledge, i.e., experimental data. However, past research was based on an assumption that error and variability behave within designer's expectations, ignoring the chance for the unexpected. Therefore, the objective of this paper is to model the unexpected failure modes in probabilistic design framework.

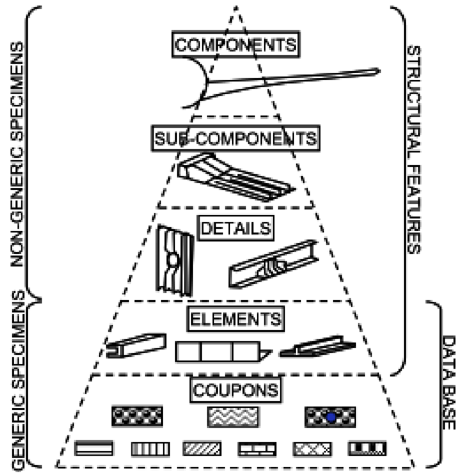

Figure 1:Building-block approach for testing aircraft structural components

Toward achieving the objective, the following steps are taken: (1) modeling an unexpected failure mode in the probabilistic design framework, (2) quantifying the impact of unexpected failure modes on reliability, and (3) quantifying the contribution of Building-Block tests to prevent unexpected failure modes from occurring in service. The key questions are as follows.

- When and how are unexpected failure modes embedded in the multi-stage design process?
- When and how do Building-Block tests uncover unexpected failure modes?

We will discuss first how an unexpected failure mode can be modeled in the probabilistic design framework in section II. Then, modeling multi-stage design and test processes is described in section III. In addition, design errors which possibly happen in each process are described and modeled along with the description of each process. In section IV, a simulation method for calculating probability of failure is explained. Section V shows an example problem and results. Finally conclusion and future work are presented in section VI.

II. Modeling unexpected failure mode

Since our objective is to quantify the effect of unexpected failure mode on probability of failure, the unexpected mode needs to be modeled in terms of uncertainty distribution, i.e., distribution of probability density function (PDF). Figure 2 illustrates a model of the unexpected failure mode depicted for a stress-strength model. First, we assume the true stress, e_{true}, is to be 100, which is unknown to the designer. Let us assume that the calculated stress by the designer, σ_{cal}, is 80, 20% off the true value due in part to an unmodeled behavior. The designer expects the error in the stress calculation, e_{exp}, to be ±10% (say uniformly distributed), and the true stress is out of designer's expected range as shown in Fig 2, In the formulation, the calculated stress, σ_{cal}, and the expected stress, σ_{exp}, can be expressed using error terms as

$$\sigma_{cal} = (1 + e_{true})\sigma_{true} \tag{1}$$

$$\sigma_{exp} = (1 + e_{exp})\sigma_{cal} \tag{2}$$

where e_{true} is the single valued true error (here -0.2) and e_{exp} is the distribution that the designer assumes. In this paper, negative error is unconservative.

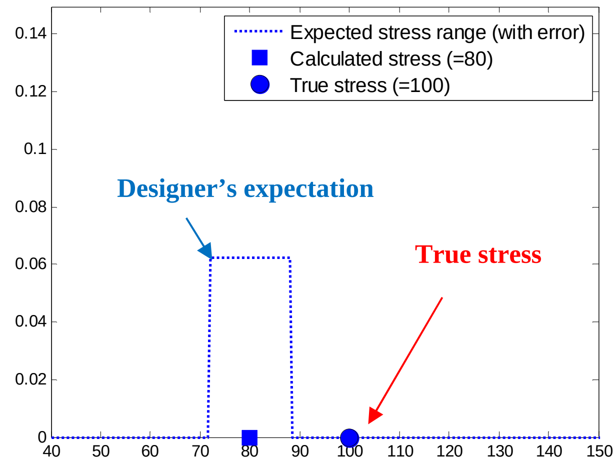

Figure 2: Unexpected failure mode

We now add material and manufacturing variability in order to illustrate the effect of the unexpected error on the probability of failure. Let the failure strength have a mean of 115 and be normally distributed with 9% coefficient of variation (COV) due to material variability. Also, let the stress be normally distributed about the mean values, such as the calculated and true values, with 5% COV due to manufacturing variability. Figs 3(a) and (b) show illustrative comparisons between the probability of failure that the designer estimates and its true value. As expected, the designer substantially underestimates the risk by ignoring the unexpected failure mode. Note that the distribution of the expected stress shown in Figure 3(a) is wider than the true stress distribution shown in Fig 3(b). This is because the expected stress distribution takes into account both the assumed distribution of the calculation error (epistemic uncertainty) and the manufacturing variability (aleatory uncertainty), while the true stress distribution considers only manufacturing variability. In this paper, the unexpected failure mode, which is unknown to designer, is modeled by generating a synthetic true error which is larger than the designer's estimate.

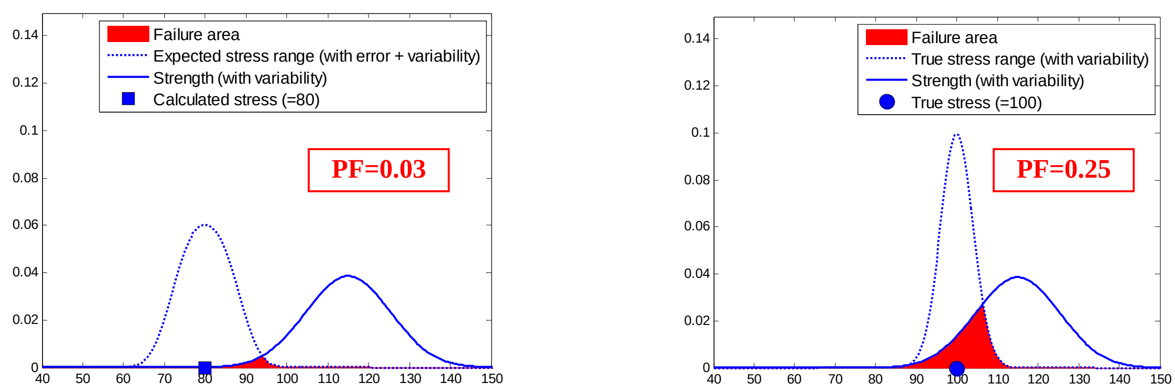

(a) Designer's expected PF **(b) True PF due to unexpected error**

Figure 3: Comparison of true and designer-calculated probabilities of failure (PF)

III. Modeling hierarchical design and test processes

In this section we describe how to model the Building-Block approach that is a synergetic process between design and test. We assume that a designer is designing an assembled structure that consists of a number of structural elements. For example, an aircraft wing or fuselage can be viewed as an assembled structure, or a subsystem. On the other hand, bolted joint, bonded joint, stiffened panel and sandwich panel can be categorized as a structural element. We include the test process at the material level, held for determining material properties, such as material strength. As a result, we have three design and test stages, i.e., assembled structure level, structural element level, and material level. In this section, possible errors associated with each process are discussed and modeled along with the description of the each process.

Figure 4 shows a flowchart of design and test processes that we modeled. It starts with the assembled structure design, where design requirements for structural elements, such as the load requirement, P_{req}, are determined. Then, the coupon test of material which is selected for the each element is held to determine the material allowable, $\sigma_{f,allow(M)}$. At the element level, the design allowable of the element, $\sigma_{f,allow(E)}$, are predicted by using failure theories, e.g., Tresca, Von-Mises, and Tsai-Wu. Once the design requirement and the design allowable of the elements are set, the design of the structural element is determined by using analytical models. Here, we assume that the cross-sectional area of the element, A_{design}, is the design parameter.

Table 1 shows a list of the possible errors modeled in the processes. For example, at the element design stage, there is the error in stress calculation, e_σ. In the same manner described in the previous illustrative example, the designed area can be expresses as

$$A_{design} = (1 + e_\sigma)\frac{SF_{(E)}P_{req}}{\sigma_{f,allow(E)}}$$

where $SF_{(E)}$ is the factor of safety on load. Note that the true stress calculation is assumed to be given by $\sigma = P/A$. Thus the stress analysis model is biased due to the error as $\sigma = (1 + e_\sigma)\, P/A$.

After designing, the element test and the assembled structure test take place to verify and certify the design. At the element test, the structure is tested to failure in order to see if it withstand the ultimate load, the expected maximum flight load (called limit load) multiplied by the factor of safety. Once the element test succeeds, the assembled structure is imposed on the ultimate load for the purpose of certification. Fails at the tests means the related design is unconservative and rejected, and then presumably would be re-designed, which is not modeled in this paper. Details of those design and test process are described in following subsections.

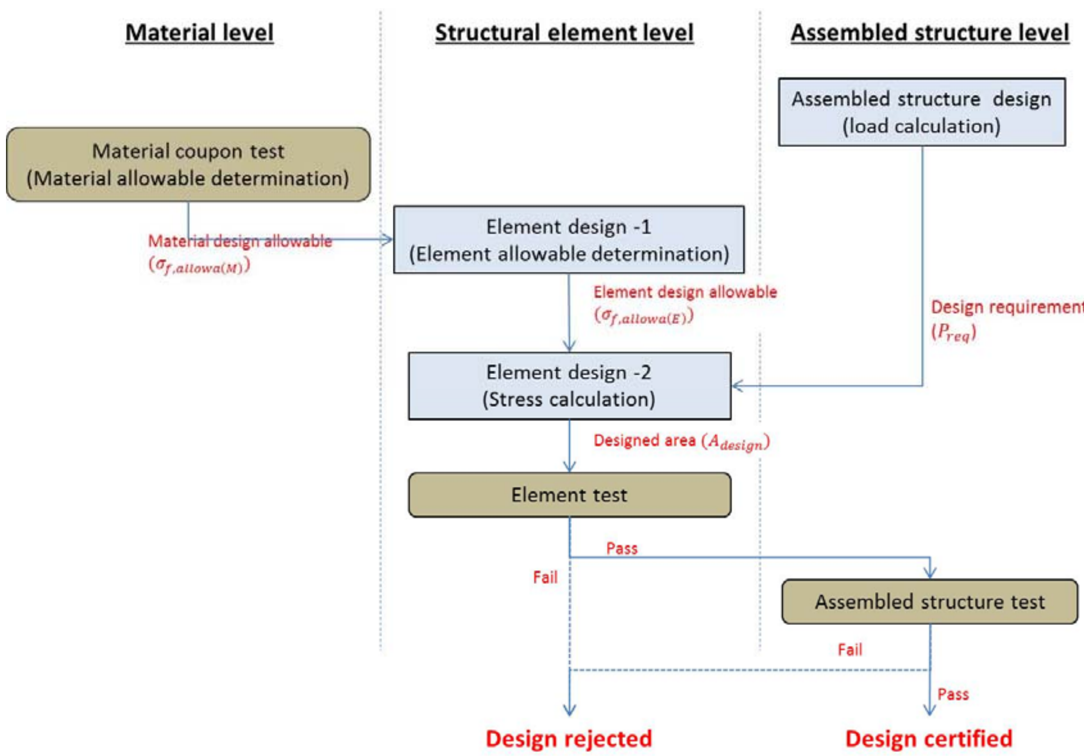

Figure 4: Flowchart of design and test processes

Table 1: List of possible errors modeled

Development Stage	Structural Complexity	Notation	Description
	Material	$e_{\sigma f(M)}$	Error in predicting material strength (failure stress)
		e_{α}	Error in failure theory
		e_{σ}	Error in stress calculation of structural element
		$e_{P,pred}$	Error in predicting flight load
		$e_{P,cal}$	Error in internal load calculation across the assembled structure
	Element	$e_{test(E)}$	Error in test configuration and measurement
	Assembled Structure	$e_{test(A)}$	Error in test configuration and measurement
Manufacturing	Element	e_A	Error in geometry (area of element) due to manufacturing

A. Assembled structure design (Load calculation)

The purpose of assembled structure design is not only to see if the designed structure satisfies its required performance but also to calculate internal loads and thus set design requirement for structural elements. The process starts with the calculation of the maximum load that an element may experience, P_{cal}, which is usually called the limit load. At this point, a designer might have errors both in flight load prediction and internal load calculation, which are denoted as $e_{P,exp}$ and $e_{P,cal}$ respectively. For example, the error in the internal load calculation may be due to an unexpected or un-modeled interaction of the element with the rest of the structure. In the same manner described in the illustrative example in the previous section, P_{cal} can be expressed by adding $e_{P,exp}$ and $e_{P,cal}$ to the true load, P_{true}.

$$P_{cal} = (1 + e_{P,pred})(1 + e_{P,cal})P_{true} \tag{3}$$

If those errors are negative, P_{cal} underestimates the true load. Finally, the required load condition for an structural element, P_{req}, is determined as

$$P_{req} = P_{cal} \tag{4}$$

B. Material coupon test (Material allowable determination)

Once the design requirement for the structural element is set, the next step is to determine the strength of a material selected for the element. A large number of coupon specimens are usually tested to failure to obtain material strength (e.g., by uniaxial tensile test) and then a probability density function (PDF) of material strength is constructed. Since the number of specimens is finite, there is an error in the PDF. Since the mean of the PDF has an error, $e_{\sigma f(M)}$, the calculated mean material strength can be obtained by adding the error to the true mean material strength, $\sigma_{f,true(M)}$ as

$$\sigma_{f,cal(M)} = (1 + e_{\sigma f(M)})\sigma_{f,true(M)} \tag{5}$$

Note that 'M' in parentheses represents 'Material level' so as to distinguish from similar notations used at the element level. There is also a corresponding error in the standard deviation of the distribution. The errors depend on the number of coupon tests and are discussed further in Appendix I.

Customarily for aircraft and aerospace applications, strength design allowable is determined as an A-basis value or B-basis value. The A-basis value is a 95% lower confidence bound for the upper 99% of a specified population, while the B-basis value is 95% lower confidence bound for the upper 90% of a specified population [12]. The former is applied to a single-point catastrophic failure, while the latter to a redundant load path. Finally the design allowable of the material is obtained as

$$\sigma_{f,allow(M)} = (1 - k_d)\sigma_{f,cal(M)} \tag{6}$$

where k_d is the knockdown factor corresponding to the choice of its design allowable (A or B-basis).

C. Element design -1 (Element allowable calculation)

Since an element is usually exposed to multi-axial stress, the design allowable obtained from uniaxial coupon tests cannot be directly used for element design. For multi-axial stress, there are several well-known failure criteria, such as Tresca, Von-Mises, or Tsai-Wu. The calculated strength of an element, $\sigma_{f,cal(E)}$, is assumed to be expressed as a function of the calculated material strength as

$$\sigma_{f,cal(E)} = (1 - e_\alpha)\alpha_{true}\,\sigma_{f,cal(M)} \tag{7}$$

where the coefficient α_{true}, representing true failure theory, is used to convert the uniaxial strength to the multi-axial strength. Since there is an error in failure theories, the calculated value is expressed by adding the error in failure theory, e_α to the true failure theory.

The sign in front of e_α is negative so that positive error implies conservative calculation. Finally by applying the knockdown factor calculated from coupon test, the design allowable of the structural element is determined as

$$\sigma_{f,allow(E)} = (1 - k_d)\sigma_{f,cal(E)} \tag{8}$$

D. Element design -2 (Stress calculation)

We assume that at element design the designer determines the cross-sectional area of structure which satisfies all the design requirements. Here, the true stress calculation is assumed to be given by $\sigma = P/A$. The stress calculation model is expressed by considering the effect of the error in calculation, e_σ, as

$$\sigma=(1+e\sigma)\ PA \tag{9}$$

Thus, the designed cross-sectional area of the element, A_{design}, is calculated by taking into account the factor of safety, SF.

$$A_{design} = (1 + e_\sigma)\frac{SF\ P_{req}}{\sigma_{f,allow(E)}} \tag{10}$$

E. Element test

After designing structural elements, element tests are held in order to verify the design, update the design allowable of the element, and redesign if needed. We assume that we construct a finite number of test specimens, $N_{E,test}$, that are nominally identical. Then, the specimens are loaded to failure. Observed element strengths are, then, converted to load tolerances of the test specimens in order to see if the designed structure meets the requirement.

Each specimen has different element strength and area due to material variability and manufacturing variability, respectively. The element strength varies about the true mean element strength, $\sigma_{f,true}$

$$\sigma_{f,test(E)} = \left(1 + v_{\sigma f}\right)\sigma_{f,true(E)} = \left(1 + v_{\sigma f}\right)\alpha_{true}\,\sigma_{f,cal(M)} \tag{11}$$

where $\sigma_{f,true(E)} = \alpha_{true} \cdot \sigma_{f,true(M)}$, and $v_{\sigma f}$ stands for variability in element strength. On top of the manufacturing variability of the element area, there might be a gap between the designed value and actual manufactured mean value (average of all the specimens). So the manufactured area of element is a function of both of variability and error

$$A_{test} = (1 + v_A)(1 + e_A)A_{design} \tag{12}$$

Moreover, there is a discrepancy in load condition between test and actual flight condition, such as boundary condition and applied load configuration; test cannot replicate 100% flight condition. In addition, there is an error in measurement. We aggregate all of these in a single error as the test error, $e_{test(E)}$, and then observed element strength, $\sigma_{f,test,obs(E)}$, is expressed as

$$\sigma_{f,test,obs(E)} = (1 - e_{test(E)})\sigma_{f,test(E)} \tag{13}$$

The sign in front of $e_{test(E)}$ is negative so positive error implies conservative calculation.

After the test, it is assumed that the minimum load tolerance value is chosen to determine whether or not the design satisfies the requirement as shown in following equations

$$P_{tol(E)} = min\left(A_{test_1}\sigma_{f,test(E)_1}, A_{test_2}\sigma_{f,test(E)_2}, \dots\ A_{test,N}\sigma_{f,test(E)_N}\right) \quad \text{where N} = N_{E,test} \tag{14}$$

Criterion of element test
Element design is verified if $P_{tol(E)} \geq SF\ P_{req}$
Element design is NOT verified if $P_{tol(E)} < SF\ P_{req}$

where $P_{tol(E)}$ is the load tolerance which is estimated by test results.

F. Assembled structure test

Once the element design is verified, it is a time for the assembled structure test for the purpose of certification. In reality, assembled structure test cannot proceed unless all of elements have completed their verification. In this study, we model only one representative element for the sake of simplicity. This means that we model no failure mode at assembled level due to interaction among elements, e.g., geometrical mismatch.

We assume that only one test specimen is constructed for certification. The load imposed on the assembled structure is the ultimate load, obtained by multiplying limit load by the factor of safety. If the assembled structure withstands the ultimate load without failure, the design passes certification. Similar to the element test, a discrepancy in test configuration from actual flight condition and an error in measurement are taken into account in the formulation of actual imposed ultimate load, P_{ULT}, as

$$P_{ULT} = (1 - e_{test(A)})SFP_{calc} \tag{15}$$

Criterion of assembled structure test
Certification passes if $P_{tol(E)} \geq P_{ULT}$
Certification fails if $P_{tol(E)} < P_{ULT}$

IV. Simulation procedure

A. Examining all possible design outcomes including unexpected failure mode

From a risk-decision point of view, for example for a project manager who is responsible for risk control, it is important to examine all possible design outcomes for given a design philosophy and requirements, and the variation of related reliability. Let us assume that we have 1,000 designers who all develop the same structure using the same design philosophy, such as selection of allowable, factors of safety, and the number of tests. They follow exactly the same procedure previously described. However, each will have different errors in their calculation and different test specimens at the tests due to manufacturing and material variability. Also, some of them would have substantially large errors, i.e., unexpected failure modes. As a result, they will end up with different designs, as well as different design allowables. In this section, a simulation procedure to examine possible design outcomes and their reliability is described.

Figure 5 shows the simulation procedure. First, the bounds of the each design error that the designers expect are set. It is assumed that all the designers have the same bounds. Second, the true design errors are randomly generated within the expected bounds. If the unexpected failure modes exist, the values of unexpected errors are deterministically set out of the bounds. Here, we model a probability that the designers have an unexpected failure mode, for the purpose of reflecting reality. For example, if the probability is 1 in 100 and 1000 possible outcomes are examined, 10 possible design outcomes have the unexpected failure mode. For constructing the test specimens, true values of variability in manufacturing and material property are also randomly generated following given distributions.

Third, all the design and test processes are simulated as described in the previous section. The outputs of the simulation are the designed cross-sectional areas and the test results (pass or fail). Finally, with the designed areas, the related true probability of failure and the designer's estimated probability of failure are calculated. Note that the true probability of failure is unknown to the designers. The designer's estimated probability of failure takes into account the effect of the all possible design errors. Limit state functions for the probabilities of failure are described in following subsections. For calculating the probabilities of failure, we deploy separable Monte Carlo Simulation [13]. Those simulation processes are repeated N_{design} times to examin N_{design} possible design outcomes.

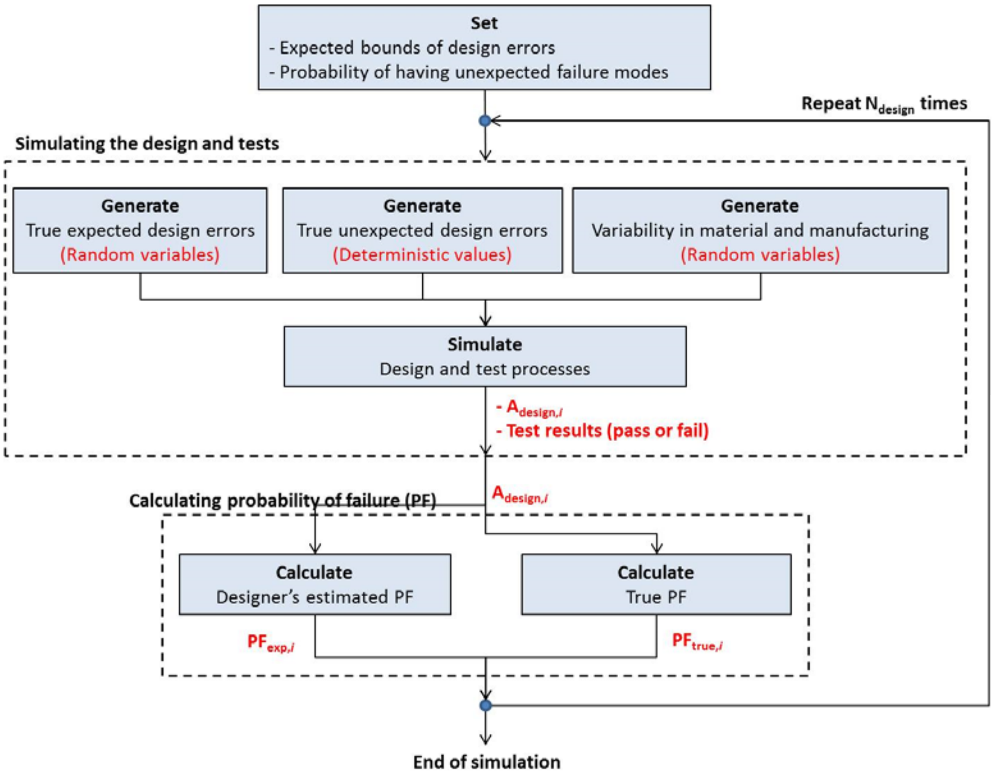

Figure 5: Simulation flowchart for possible design outcome

B. Limit state formulation for probability of failure

(1) Estimated probability of failure

Since the designer does not know the true error values, he or she calculates the probability of failure of the structure based on their assumed error bounds. In addition to errors, the probability of failure depends on variability in material properties, loads, and geometry. The formulates of the limit state function defining failure is based on the expected element strength, $\sigma_{f,exp(E)}$, and the expected element stress, σ_{exp}.

$$G = \sigma_{f,exp(E)} - \sigma_{exp} \tag{16}$$

$\sigma_{f,exp(E)}$ can be written by adding a term of material variability to Eq. (7)

$$\sigma_{f,exp(E)} = (1 + v_{\sigma f})(1 - e_{\alpha,exp})\alpha_{true}\sigma_{f,cal(M)} \tag{17}$$

As previously discussed in Section III, $e_{\alpha,exp}$ depends on the number of coupon tests and the distribution of true material strength. For more details, readers are referred to Appendix I. The expected stress σ_{exp} can be obtained by modifying the stress calculation formulation in Eq. (9). Also variability in the calculated load, v_P, and the area of structure, A_{design}, are taken into account.

$$\sigma_{exp} = (1 + e_{\sigma,exp})\frac{(1 + v_P)(1 + e_{P,pred,exp})(1 + e_{P,cal,exp})P_{cal}}{(1 + v_A)(1 + e_{A,exp})A_{design}} \tag{18}$$

Note that errors in the estimated element strength and stress, $e_{\alpha,exp}$, $e_{\sigma,exp}$, $e_{P,pred,exp}$, $e_{P,cal,exp}$, and $e_{A,exp}$, are not the same as the associated values of true errors used in the simulation. Those estimated errors are random variables which follow certain properties of PDF distribution that the designer expects. In this paper all the expected errors are assumed to follow uniform distribution as shown in the illustrative example in section I.

(2) True probability of failure

Similarly, the limit state function for true probability of failure (unknown to the designer) is expressed with the true element strength, $\sigma_{f,true(E)}$, and the true element stress, σ_{true}.

$$G = \sigma_{f,true(E)} - \sigma_{true} \tag{19}$$

Unlike the limit state for the estimated probability of failure, both of $\sigma_{f,true(E)}$ and σ_{true} do not include any error except for the element area which has the manufacturing error. The true stress and true element strength can be expressed by only true values as shown in Eq. (20) and (21).

$$\sigma_{f,true(E)} = (1 + v_{\sigma f})\alpha_{true} \cdot \sigma_{f,true(M)} \tag{20}$$

$$\sigma_{f,allow(E)} = \frac{(1 + v_P)P_{true}}{(1 + v_A)(1 + e_{A,true})A_{design}} \tag{21}$$

V. Example problem and result

A. Example problem

Table 2 shows the true variables which are used in example problem. They are unknown to designers. First, flight load is defined as the maximum load that an aircraft may experience in its lifetime. Therefore, the probability of failure discussed in this section is the probability of failure in the lifetime (not per flight). The distribution of the maximum load assumed to follow Type I extreme value distribution with 10% COV. The distribution parameters are selected so that the probability that maximum load exceeds a given limit load is 1/1000, meaning that if there are 1000 aircrafts in the fleet, one of them will experience the limit load [14]. Details of the procedure to determine the parameters of the maximum load distribution are given in Appendix II.

Material strength is assumed to be normally distributed. The failure theory adjustment, represented by α_{true}, is assumed to be unity for the sake of simplicity. Error in element area e_A follows uniform distribution. The probability of having the unexpected modes are based on personal communication with engineers from Boeing and Airbus, and their estimate is about one such failure per 100 elements. In addition, we assume that because of the multitude of elements, one airplane in 10 will have an unexpected failure mode. So that the probability having the unexpected failure mode is 1 in 10 design outcomes.

Table 3 shows the design margins that the designer follows and the number of tests. Three element tests and one assembled structure test are held. Table 4 is the list of designer's expected error bounds as well as the unexpected error value produced. In this example, we have only one unexpected error in the element stress calculation. The value of the unexpected error is fixed, and examined with various values from -0.1 to -0.3. For example, -0.25 error means 25% off the true value in unconservative direction. In the simulation, 1,000 possible design outcomes (each corresponding to one set of true errors) are examined, so that the unexpected failure mode lies in 100 possible design outcomes. In Separable Monte Carlo Simulation, 10,000 random samples for errors and variability are generated. Table 5 shows the simulation parameters.

Table 2: True design variables

Variable	Type of distribution	Property
Maximum flight load (P_{true})	Type I extreme value distribution	Location parameter = 63.9 Scale parameter = 5.2 (True limit load = 100 [*1])
Material strength ($\sigma_{f,true(M)}$)	Normal distribution	mean: 150 COV: 10%
Error in element area (e_A)	Uniform distribution	± 5% bounds
Failure theory (α_{true})	-	$\alpha_{true} = 1$
Experimental error (e_{test})	-	$e_{test(E)} = 0$ $e_{test(A)} = 0$
Probability of having an unexpected failure mode	-	1 in 10 design outcomes

[*1] Distribution parameters are selected so that the probability that the maximum flight load exceeds the true limit load is 1 n 1000.

Table 3: Design Margin and number of tests

Notation	Description	Value
SF	Factor of safety at element design	1.4
k_d	Knockdown factor (Material allowable selection)	kd≈0.156 based on B-basis value with 100 coupon test specimens
-	Number of coupon tests	100
N_E	Number of element tests	3
-	Number of assembled structure tests	1

Table 4: List of modeled errors

Development Stage	Structural complexity	Notation	Designer's expectation (Uniform Distribution)	Unexpected error
	Material	$e_{\sigma f(M)}$	Depending on test result *1	N/A
		e_{α}	[-0.1 0.1]	N/A
		e_{σ}	[-0.1 0.1]	Varied from -0.1 to -0.3
		$e_{P,pred}$	[-0.1 0.1]	N/A
		$e_{P,cal}$	[-0.1 0.1]	N/A
	Element	$e_{test(E)}$	[-0.01 0.01]	N/A
	Assembled structure	$e_{test(A)}$	[-0.01 0.01]	N/A
Manufacturing	Element	e_A	[-0.05 0.05]	N/A

*1 For more detail, see Appendix I.

Table 5: Setting for Simulation

Description	Value
Number of simulated design outcomes	1,000
Number of simulated design outcomes which have the unexpected failure mode	100 out of above 1,000
Number of samples in Separable Monte Carlo simulation	10,000 samples for each random variable

B. Result and discussion

First, we pick up the results of $e_{\sigma,true}$= -0.25 case to discuss in detail of the unexpected failure mode and the trend of the probabilities of failure associated with the possible design outcomes. Table 6 shows the calculated probabilities of failure and test results of $e_{\sigma,true}$= -0.25 case. Table 7 shows designer's estimated probability of failure that ignores the existence of the unexpected failure modes. It can be seen that the average (over 1,000 design outcomes) designer-estimated probability of failure (4.53×10^{-5}) is higher than the true value which does not include the effect of unexpected failure mode (1.48×10^{-7}). This is because taking into account all possible epistemic uncertainties makes distributions of uncertainties wider than true, resulting in higher estimate of probability of failure. We also see that the -25% error assumed for the unexpected failure mode in 10% of the airplanes raises the risk. Probability of failure is increased by more than one order of magnitude (from 1.48×10^{-7} to 5.97×10^{-6}).

At the element test, 98% of the design outcomes with the unexpected failure mode failed, resulting in significant improvement of the probability of failure (from 5.97×10^{-6} to 7.12×10^{-8}). This result happened because of following reasons. Since the effect of the factor of safety considered in the design process is canceled by the ultimate load, the essential safety factor for the test is reduced from to 1.19, which is only from the knockdown factor considered for the strength allowable (k_d≈0.156). In addition, the 25% unconservative error makes the factor of safety even smaller to 0.89. Finally, by taking the minimum values of strength of the test specimens, most of the unexpected failure modes are detected by the element test. Fig 6 shows the histogram of the designed cross-sectional area. It can be seen that the design outcomes with the unexpected failure modes has substantially small areas compared to the normal designs. Presumably these designs that failed would be re-designed, but this is not included in the present simulation. Adversely, this severe criterion even screened out 29% of the normal designs without the unexpected failure mode (262 designs). As shown in Fig 6, some of the normal designs have the relatively small areas as the designs with the unexpected failure mode. This is because of the fact the there are a sampling error to determine the material strength allowable from the coupon tests, and the error in stress calculation to determine the cross-sectional area.

After the assembled test, one design outcomes with the unexpected failure mode survived, while additional 31 normal designs failed. The applied load at the assembled structure test is identically the same as the load criterion of the element test. Also, it is assumed that there is no unexpected error embedded in assembled structure level. Therefore, the number of fails at the assembled structure test is fewer than the element test. Only difference from the element test is variability in the element strength and the structural area. Consequently, the probability of failure of the designs that pass the assembled structure test (7.48×10^{-8}) is reduced by two orders of magnitude from the initial one ($5..97\times10^{-6}$), and it is even smaller than the case where no unexpected failure mode exists (1.48×10^{-7}).

Table 6: True probability of failure (PF) and test result for $e_{\sigma,true}$= -0.25

Design outcomes		mean of True PF *1	No. of design outcomes *2
All design outcomes		5.97×10^{-6} (15.7)	1,000
Design outcomes having unexpected mode		5.84×10^{-5} (5.0%)	100
Design outcomes not having unexpected mode		1.48×10^{-7} (17.5)	900
	Pass	7.12×10^{-8} (19.1)	640 (2)
	Fail	1.65×10^{5} (5.5)	360 (98)
	Pass	7.48×10^{-8} (18.5)	609 (1)
	Fail	0 (N/A)	31 (1)

*1 Number in parentheses shows design outcomes having unexpected failure mode

*2 Number of parentheses shows coefficient of variation of probability of failure

Table 7: Designer's expected probability of failure (PF)

Designer-expected PF
mean: 4.53×10^{-5}
COV: 1.41

Next, we looked at the result in terms of distribution of probability of $e_{\sigma,true}$= -0.25 case. Figure 7 shows the histogram of the probability of failure of all design outcomes. As seen in the histogram, most of the cases lie on fairly small probability of failure including 922 zero values. These zero values are due to the finite sample of Separable Monte Carlo Simulation ($10{,}000\times10{,}000$ samples), but they correspond to very low probabilities. Thus, about 90% of the designs are below the mean of the true probability of failure. In the Fig 8, the probability of failure of the design outcomes which contain the unexpected failure mode is distinguished from the normal designs without the unexpected failure mode. It can be seen that the mean values of the probability of failure shown in Table 6 is substantially influenced by the existence of the unexpected failure mode. Figures 9 and 10 show the histogram after the element and the assembled structure tests, respectively. It can be seen that the tests do well to discover unconservative designs.

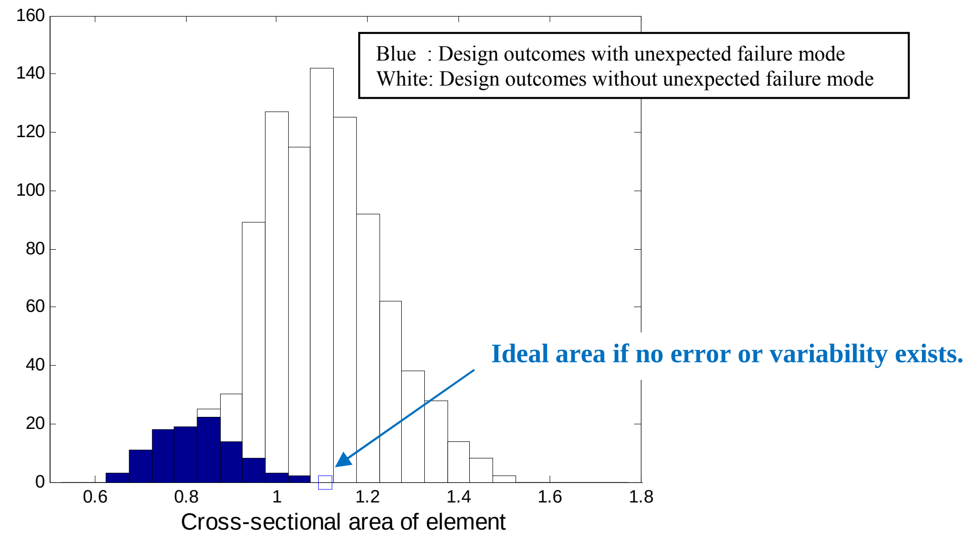

Figure 6: Histogram of designed cross-sectional area of element

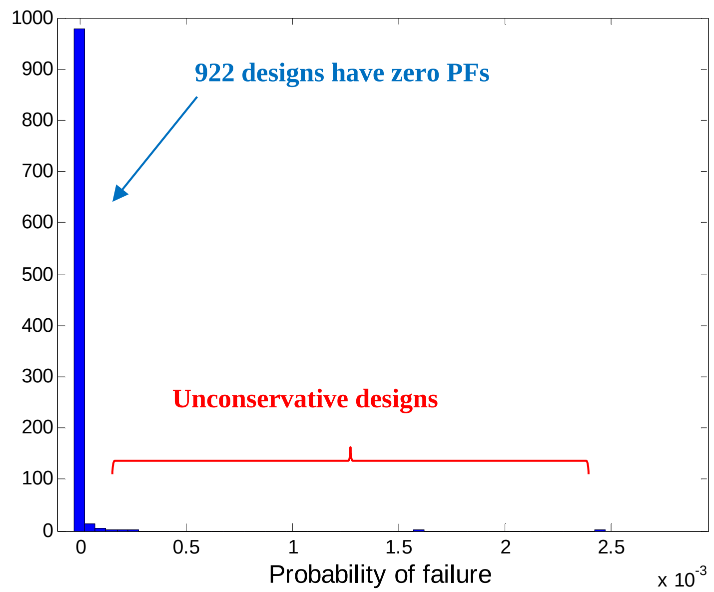

Figure 7: Histogram of probability of failure
(All 1,000 design outcomes)

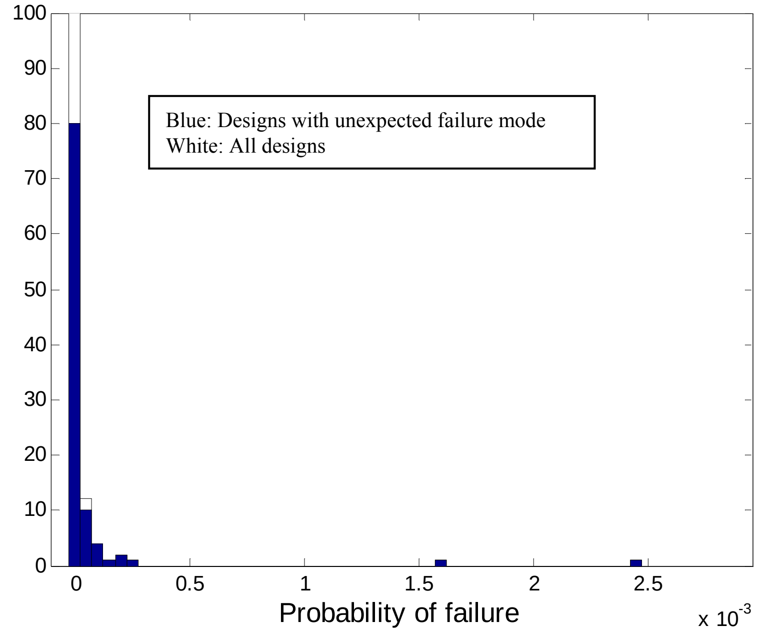

Figure 8: Histogram of probability of failure
(100 Design outcomes with unexpected mode)

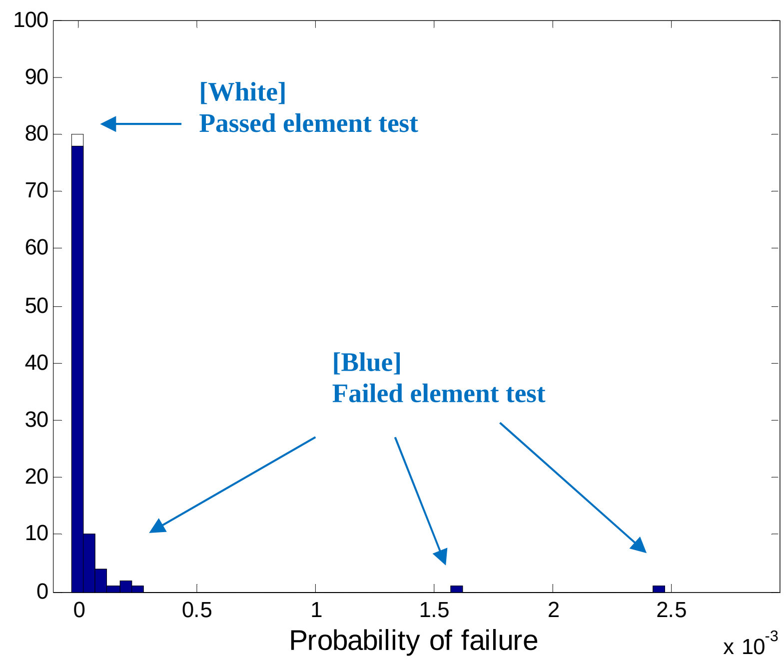

Figure 9: Histogram of probability of failure after element test
(100 Design outcomes with unexpected mode)

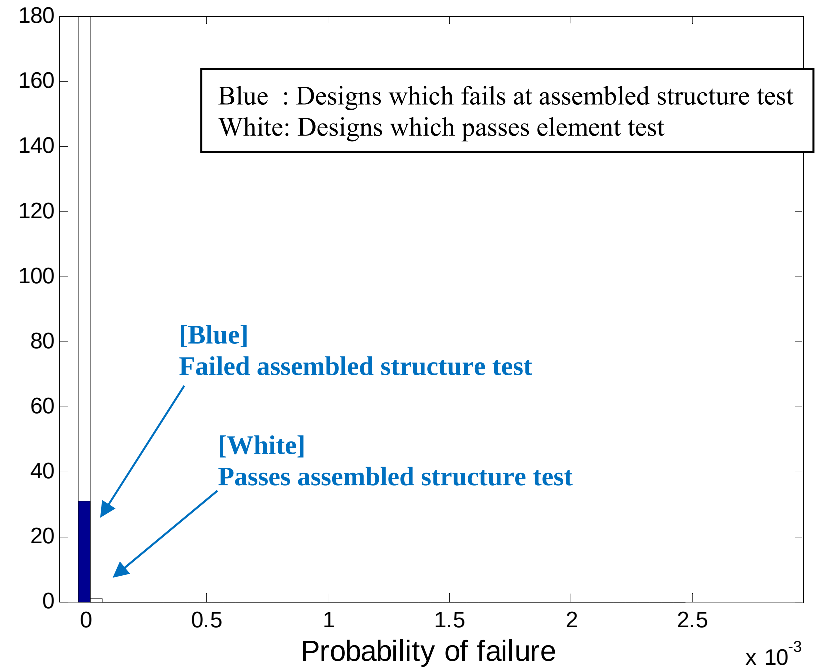

Figure 10: Histogram of probability of failure after Assembled structure test (All 1,000 design outcomes)

Second, we examine the effect of the magnitude of the unexpected error. Figure 11 shows the comparison of probability of failure with respect to the magnitude of the unexpected error. Figure 12 shows the number of survivors after the tests. Before the tests, the true probability of failure increases as the magnitude of error is increased (from -0.1 to -0.3). For any case, it can be seen that tests works well to reduce the probability of failure. Even the error is small (-0.1 error case), improvement of reliability is done by one order of magnitude. When the error is large, for example -0.3 error case, the probability of failure is reduced by three orders of magnitude.

It can be seen that the probabilities of failure after the tests zigzag with respect to the error. This is mainly due to the noise of Monte Carlo simulation. For any error case, the probabilities of failure after the tests become smaller than the probability of failure of the normal design outcomes without the unexpected failure modes. The probability of failure improvements for all cases are done by about one order of magnitude and converged to 10^{-8} level regardless of the number of the unexpected failure modes remaining (Fig 12). When the error is small, many unexpected failure modes survive. But, they do not have a significant effect on the probability of failure, because the probabilities of failure of those unexpected failure modes are substantially small (10^{-8} level). On the other hand, when the error is large, the related probability of failure is higher (e.g., 10^{-4} level for -0.3 error case). However, all or the most of the unexpected failure modes are discovered by the tests for -0.3 and -0.25 cases. Note that for -0.25 error case the probability of failure of the survived design with the unexpected failure mode is zero.

It is shown that Building-Block test significantly contributes to compensate for the unexpected failure mode and reduce the probability of failure. Especially, Building-Block test with the severe load condition, i.e., ultimate load, essentially work well no matter how large the unexpected error is.

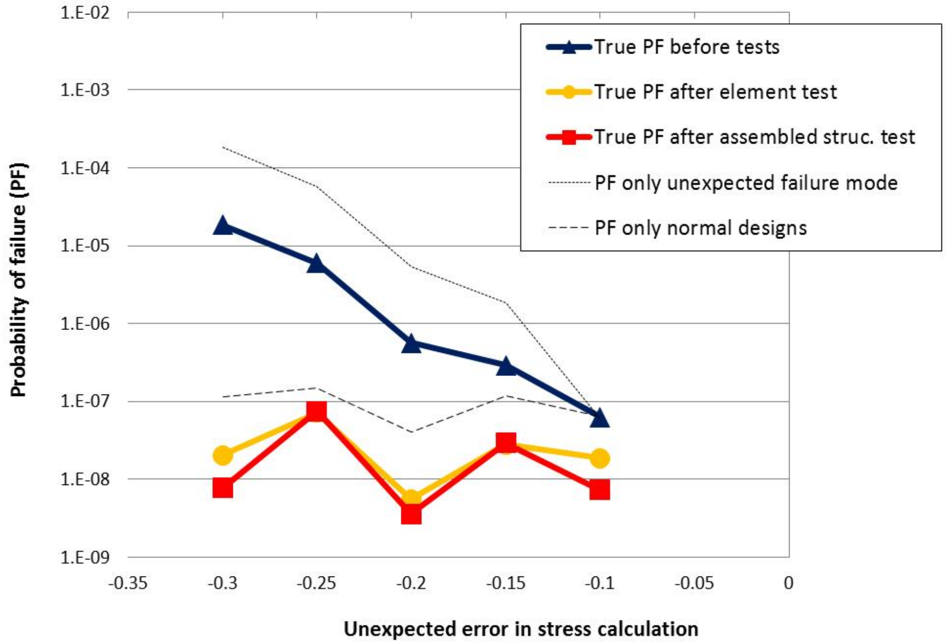

Figure 11: Probability of failure comparison with respect to magnitude of unexpected error

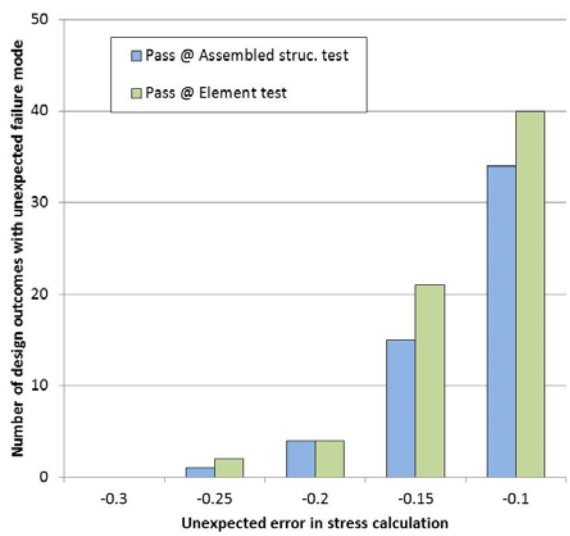

Figure 12: Number of survivors after tests respect to magnitude of unexpected error

VI. Conclusion

We proposed a modeling method of unexpected failure mode within the hierarchical design and test processes including uncertainties (errors and variability). With the example problem, we showed that ignoring the effect of the unexpected failure mode leads a substantial unconservative estimate of probability of failure by orders of magnitude. In addition, we showed that post-design tests, Building-Block test, significantly contribute to discovering the unexpected failure modes and reducing the probability of failure. By varying the magnitudes of unexpected design error, it is found that the Building-Block test works well regardless of the magnitude of the unexpected errors.

Poste-design tests are also known as a process that reduces epistemic uncertainties using statistic techniques, such as Bayesian inference. For future work, we will integrate the uncertainty reduction process after tests into the current model. Then, we will examine how the uncertainty reduction along with redesign process works for the unexpected failure mode.

.

Appendix I. Error in calculated material strength

Let the number of coupon test N_M. Sample mean of the observed material strength, $\mu_{\sigma f,test}$, is calculated from well-known equation

$$\mu_{\sigma f,test} = \frac{1}{N_M}\sum_{i=1}^{N_M}\sigma_{f,test\_i(M)} \tag{A-1}$$

where $\sigma_{f,test\_i(M)}$ is observed material strength of ith test specimen. Standard deviation of the observed material strength, $STD_{\sigma f,test}$, is obtained as

$$STD_{\sigma f,test} = \sqrt{\frac{1}{N_M - 1}\sum_{i=1}^{N_M}(\sigma_{f,test_{i(M)}} - \mu_{\sigma f,test})^2} \tag{A-2}$$

Since the number of coupon test is finite, both of $\mu_{\sigma f,test}$ and $STD_{\sigma f,test}$ are not exactly the same as true values, meaning both of them have errors. Therefore, possible mean and possible standard deviation of material strength need to be estimated; the mean and the standard deviation of the sampled material strength can be estimated as individual PDF distribution. Let distributions of the estimated mean and the estimated standard of the observed material strength deviation denoted as $\mu_{\sigma f,est}$ and $STD_{\sigma f,est}$.

It is known that if the distribution of true material strength follows normal distribution, the estimated mean of the observed material strength also follows normal distribution. [15]. $\mu_{\sigma f,est}$ can be expressed

$$\mu_{\sigma f,est} \sim N\left(\mu_{\sigma f,test}, \frac{STD_{\sigma f,test}}{\sqrt{N_M}}\right) \tag{A-3}$$

Also, the estimated standard deviation of observed material strength, $STD_{\sigma f,est}$, follows chi-distribution of order of N_M-1.

$$f_{\mu_{\sigma f,est}}\left(STD_{\sigma f,est}\right) = \chi^2(x^2|N_M - 1)2x \text{ where } x = \frac{\sqrt{N_M - 1}}{STD_{\sigma f,test}}STD_{\sigma f,est} \tag{A-4}$$

where $f_{\mu_{\sigma f,est}}(.)$ represents PDF function and $\chi^2(x|N_M - 1)$ is chi-square distribution with N_M-1 degrees freedom.

Appendix II. Maximum load distribution

The maximum load that an aircraft experiences in the lifetime is assumed to follow Type I extreme value distribution, usually called Gumbel distribution, having 10 % COV. We also assume that there are 1,000 aircrafts in the fleet and one of them will encounter the limit load over their lifetime. Cumulative distribution function (CDF) of Type I extreme value distribution, $F_X(x)$, is characterized with two parameters, such as location parameter, μ, scale parameter, β.

$$F_X(x) = \exp(-\exp(-\frac{x-\mu}{\beta})) \tag{B-1}$$

Mean and standard deviation are

$$\begin{aligned} &\text{Mean:} \quad \mu + \beta\gamma \\ &\text{Standard deviation:} \quad \pi\beta/\sqrt{6} \end{aligned} \tag{B-2}$$

where γ is Euler–Mascheroni constant (≈0.577).

Since COV is 10%, from Eq. (B-2), the distribution parameters can be reduced to one parameter as shown in Eq. (B-3)

$$0.1 = \frac{\pi\beta/\sqrt{6}}{\mu + \beta\gamma} \quad \rightarrow \quad \mu = (10/\sqrt{6} - \gamma)\beta \tag{B-3}$$

For given limit load, P_{LMT}, and given probability (=1/1000) which is equal to CDF value, the parameter β can be determined by Eq. (B-4) and μ is calculated by Eq. (B-3).

$$1/1000 = \exp(-\exp(-\frac{P_{LMT} - (10/\sqrt{6} - \gamma)\beta}{\beta})) \tag{B-4}$$

Acknowledgments

This research was partly supported by National Science Foundation (Grant CMMI-0927790). The authors gratefully acknowledge this support.

References

[1] S. Pitt and R. Jones, "Multiple-site and widespread fatigue damage in aging aircraft," Engineering Failure Analysis, Vol. 4 (4), 1997, pp. 237–257

[2] MIL-HDBK-17-3F, "Department of Defense Handbook Composite Materials Handbook," Vol. 3, 17 June, 2002.

[3] Rouse, M., Jegley, D. C., McGowan, D. M., Bush, H. G., "Utilization Of The Building-Block Approach In Structural Mechanics Research," 46th AIAA/ASME/ASCE/AHS/ASC Structures, Structural Dynamics & Materials Conference, 18 - 21 April 2005, Austin, Texas

[4] Fawcett, A., Trostle, J., Ward, S., "777 Empennage Certification Approach," 11th International Conference on Composite Materials (ICCM-11), Australia, July 14-18, 1997

[5] D.M. Frangopol, and K. Maute, "Life-cycle reliability-based optimization of civil and aerospace structures," Computer and Structure, 81, 2003, pp. 397–410

[6] Acar, E., Kale, A., Haftka, R. T., and Stroud, W. J., "Structural Safety Measures for Airplanes," Journal of Aircraft, Vol. 43, No. 1, 2006, pp. 30–38.

[7] Acar, E., Kale, A., and Haftka, R. T., "Comparing Effectiveness of Measures that Improve Aircraft Structural Safety," Journal of Aerospace Engineering, Vol. 20, No. 3, 2007, pp. 186–199.

[8] An, J., Acar, E., Haftka, R. T., Kim, N. H., Ifju, P. G., and Johnson, T. F., "Being Conservative with a Limited Number of Test Results," Journal of Aircraft, Vol. 45, No. 6, 2008, pp. 1969–1975.

[9] Acar, E., Haftka, R. T., Kim, N., Turinay, M., Park, C., "Reliability-based Structural Design of Aircraft Together with Future Tests," 12th AIAA Non-Deterministic Approaches Conference, Orlando, FL, 2010

[10] Villanueva, D., Haftka, R.T., Sankar, B.V., "Including Future Tests in the Design and Optimization of an Integrated Thermal Protection System," 12th AIAA Non-Deterministic Approaches Conference, Orlando, FL, 2010

[11] Urbina, A., and Mahadevan, Sankaran., "Resource Allocation Using Quantification of Margins and Uncertainty," 12th AIAA Non-Deterministic Approaches Conference, Orlando, FL, 2010, AIAA-2010-2510

[12] MIL-HDBK-17-1F, "Department of Defense Handbook Composite Materials Handbook," Vol. 1, 17 June, 2002.

[13] Smarslok, B.P., Haftka, R.T., and Kim, N.H. "Taking Advantage of Separable Limit States in Sampling Procedures," 47th AIAA/ASME/ASCE/AHS/ASC Structures, Structural Dynamics, and Materials Conference, Newport, RI, May 2006

[14] Acar, Erdem., Haftka, Raphael T., Kim, Nam-Ho., Turinay,. Merve, and Park, Chanyoung., "Reliability-Based Structural Design of Aircraft Together with Future Test," 13th AIAA/ISSMO Multidisciplinary Analysis and Optimization Conference, Fort Worth, Texas, Sept. 13-15, 2010

[15] C. Park, T. Matsumura, R. T. Haftka, N. H. Kim, and E. Acar, "Modeling the effect of structural tests on uncertainty in estimated failure stress" 13th AIAA/ISSMO Multidisciplinary Analysis and Optimization Conference, Fort Worth, Texas, Sept. 13-15, 2010